



Decoupling through input–output blending

Tamás Baár & Tamás Luspay

To cite this article: Tamás Baár & Tamás Luspay (2020): Decoupling through input–output blending, *International Journal of Control*, DOI: [10.1080/00207179.2020.1773540](https://doi.org/10.1080/00207179.2020.1773540)

To link to this article: <https://doi.org/10.1080/00207179.2020.1773540>



Accepted author version posted online: 23
May 2020.
Published online: 04 Jun 2020.



Submit your article to this journal [↗](#)



Article views: 15





View related articles [↗](#)



View Crossmark data [↗](#)



Decoupling through input–output blending

Tamás Baár  and Tamás Luspay 

Systems and Control Lab, Institute for Computer Science and Control, Budapest, Hungary

ABSTRACT

The paper presents a novel decoupling method, based on blending the input and output signals of linear dynamical systems. For this purpose, blend vectors are introduced and calculated such that the minimum sensitivity of the controlled mode is maximised, while the worst case gain of the other subsystems is minimised from the blended input to the blended output. The problem is transformed to a standard optimisation program subject to Linear Matrix Inequality constraints. An arising rank constraint is resolved by an alternating projection scheme. The method is presented based on the decoupling of a single mode, but the extension to decouple multiple modes is also discussed. Numerical examples are given to validate the method and to illustrate how the proposed approach can be applied for control engineering problems.

ARTICLE HISTORY

Received 16 September 2019
Accepted 18 May 2020

KEYWORDS

Decoupling; minimum sensitivity; linear matrix inequality; mode control

1. Introduction

In the control of multivariable complex systems, it is often desirable to ease the complexity of the underlying analysis or synthesis problem. In the vast field of large-scale dynamical systems, many approaches have been developed in the past decades. These methods can be categorised into three main groups (Bakule, 2008). Decentralisation aims for separate control design processes and their independent implementation. Decomposition aims for reducing the computational complexity by breaking the system into subsystems. Model reduction seeks for an approximate dynamical description, with lowered complexity.

The paper focuses on the decoupling (or decomposition) of dynamical systems, where our general aim is to control a certain fraction of the system, without affecting other parts. This objective is in line with the recent trends of systems- and control engineering aiming for the design of structured controllers for complex systems (Apkarian et al., 2015).

The decoupling control design has an extensive literature, and most of the papers are focusing on the input–output decoupling of a system. Stoyle and Vardoulakis (1979) design a suitable state feedback, while Marinescu (2009) achieves decoupling through a model-matching problem. According to the work of Lin and Wu (2001), a decoupling controller can also be designed by first diagonalising the plant by means of a precompensator and by synthesising a controller for the diagonalised plant. A further approach has been developed for linear parameter varying systems in Mohammadpour et al. (2011).

In recent years, various approaches were introduced in order to assure decoupled control of selected dynamical modes of a system. The common point of many of these methods is that they introduce input and output blending vectors to decouple modes and reduce the control design into a Single

Input Single Output (SISO) problem accordingly. Danowsky et al. (2013) determine an optimal blend for the measurements which assures the isolation of the selected mode. Simultaneously they compute an optimal blend for multiple control inputs to suppress the targeted mode via a negative optimal feedback, while minimising the control's effect on other modes. Pusch (2018) and Pusch and Ossmann (2019) introduce a joint \mathcal{H}_2 norm-based input and output blend calculation method which assures the controllability, observability and the independent control of selected modes. Pusch et al. (2019) takes this approach further and applies the method to the design of a gust load alleviation system on an experimental flexible wing. The \mathcal{H}_2 norm-based blend calculation technique is extended to undamped and unstable modes, where a structured controller is designed to suppress unstable wing oscillations on a flexible wing flutter demonstrator aircraft (Pusch et al., 2019).

The current paper presents a novel sensor and actuator blending approach for linear time invariant (LTI) systems, in order to assure decoupled control of individual modes with simple SISO controllers. Our approach is based on the \mathcal{H}_- index and the \mathcal{H}_∞ norm of dynamical systems. The \mathcal{H}_- index is a sensitivity measure widely used in fault detection, based on the smallest singular value of a transfer function matrix over a given frequency range (Liu et al., 2005). By its maximisation between given inputs and outputs, the system's sensitivity can be increased. Oppositely, the \mathcal{H}_∞ norm defines the maximal singular value of a transfer function matrix and it is mainly used in robust analysis and synthesis problems (Skogestad & Postlethwaite, 2007). By minimising the \mathcal{H}_∞ norm, the maximum sensitivity of the transfer function matrix is reduced. The present approach seeks input and output blend vectors which are maximising the sensitivity for a given mode, while minimising it for another one. This way, decoupling can be achieved and conse-

quently a suitably designed control law will affect one mode, while leaving unattained the other one(s).

A previous, preliminary version of the paper has appeared in Baár and Luspay (2019). This paper takes one step further and offers some remedies for the shortcomings found previously. More specifically, a novel formulation of the decoupling through input–output blending is given by using the generalised Kalman–Yakubovich–Popov (GKYP) lemma. This offers a more systematic (less heuristic) framework to investigate and solve the problem. The previous approach was relying on the use of certain weighting filters, introduced in order to convert the system into a proper one. The application of the GKYP lemma allows the calculation of the \mathcal{H}_- index over a finite frequency range for strictly proper systems also. In addition, an alternating projection scheme is incorporated to handle the arising rank constraints.

The outline of the paper is as follows. Section 2 provides the necessary mathematical formulations, followed by Section 3 with the formal problem statement. The mode decoupling algorithm for single and multiple modes is presented entirely in Section 4. Numerical examples are reported in Section 5, followed by the concluding remarks.

2. Mathematical background

Basic mathematical notions and the required definitions are given in the section, which are used throughout the construction of the decoupling algorithm.

2.1 State space representation

As a starting point, we consider continuous time LTI dynamics given in the following generic state space form

$$\mathcal{P}_{n_y \times n_u} : \begin{cases} \dot{x}(t) = Ax(t) + Bu(t), \\ y(t) = Cx(t) + Du(t), \end{cases} \quad (1)$$

with the standard notations: $x \in \mathbb{R}^{n_x}$ is the state vector, $u \in \mathbb{R}^{n_u}$ is the input vector and $y \in \mathbb{R}^{n_y}$ is the output vector of the system. The system matrices are of appropriate dimensions. In addition, we assume that the system is given in the following subsystem form:

$$\begin{aligned} A &= \begin{bmatrix} A_c & 0 \\ 0 & A_d \end{bmatrix}, \quad B = \begin{bmatrix} B_c \\ B_d \end{bmatrix}, \\ C &= [C_c \quad C_d], \quad D = [D]. \end{aligned} \quad (2)$$

Under the assumption of diagonalisable A , such a representation is always achievable with the respective similarity transformation, which is generally referred as modal form (Kailath, 1980). In modal form, the A matrix has a block diagonal structure, where each block corresponds to a dynamical mode of the system. These dynamical modes can be represented by either real (\Re) or complex (with imaginary part \Im) eigenvalues λ , which determine the structure of the corresponding block of matrix $A = \text{diag}(A_1, \dots, A_n)$ as

$$A_i = \begin{cases} \lambda_i & \text{if } \Im(\lambda_i) = 0 \\ \begin{bmatrix} \Re(\lambda_i) & \Im(\lambda_i) \\ -\Im(\lambda_i) & \Re(\lambda_i) \end{bmatrix} & \text{if } \Im(\lambda_i) \neq 0. \end{cases} \quad (3)$$

Representation (2) can be considered as a special modal form, without loss of generality, where the modes are grouped together into two subsystems: one that we wish to control and another one that we wish to decouple (leave unaffected). This is a very rough formulation of the problem, which will be followed by a more precise one in the forthcoming Section 3. The subsystems are denoted by indexes $\{\cdot\}_c$ and $\{\cdot\}_d$, respectively. Note also that such a representation might be obtained differently. During the presentation of the proposed algorithm, we assume that the $\{\cdot\}_c$ subsystem contains only one mode, while the $\{\cdot\}_d$ subsystem might contain multiple modes. The possible extension when $\{\cdot\}_c$ contains multiple modes is discussed in Section 4.3. Finally, note that, the given representation is not decoupled, as (2) shows couplings between the subsystems through the B , C and D matrices.

In addition, the transfer function matrix representation is given by

$$\mathcal{G}(s) = \sum_{i \in \{c,d\}} \{C_i(sI - A_i)^{-1}B_i + D/2\} = \mathcal{G}_c(s) + \mathcal{G}_d(s), \quad (4)$$

where $\mathcal{G}_c(s)$ and $\mathcal{G}_d(s)$ are the transfer functions of the subsystems to be controlled and decoupled, respectively, with the standard notation of s being the Laplace variable and I being the identity matrix.

2.2 Dual system

Assume that the system $\mathcal{P}_{n_y \times n_u}$ is given in state space form by (1). According to Kwakernaak and Sivan (1972), the state space matrices of the dual system $\tilde{\mathcal{P}}_{n_u \times n_y}$ are

$$\tilde{A} = A^T, \quad \tilde{B} = C^T, \quad \tilde{C} = B^T, \quad \tilde{D} = D^T. \quad (5)$$

This dual representation has a favourable property, which will be used throughout the paper. Namely, the input–output norm of the system is preserved, while the input and output dimensions are interchanged. In the paper, we will make extensive use of this fact.

Furthermore, one can introduce the tall, square and wide notations for the $\mathcal{P}_{n_y \times n_u}$ system (Li & Liu, 2010). A system is called tall when the number of outputs is higher than the number of inputs, and oppositely, it is called wide when $n_u > n_y$. We say that the system is square if $n_u = n_y$. It follows immediately that if $\mathcal{P}_{n_y \times n_u}$ is wide, then $\tilde{\mathcal{P}}_{n_u \times n_y}$ is tall.

2.3 Minimum sensitivity

In the paper, we will adopt a notion from the Fault Detection Filtering (FDI) literature to characterise the minimum sensitivity of a system (see i.e. Wang et al. (2007) and Glover and Varga (2011)). More precisely, we will use the so called \mathcal{H}_- index, defined as

$$\|\mathcal{G}_c(s)\|_-^{[0, \bar{\omega}]} := \inf_{\omega \in [0, \bar{\omega}]} \underline{\sigma}[\mathcal{G}_c(j\omega)], \quad (6)$$

with $\underline{\sigma}$ denoting the minimum singular value and $\bar{\omega}$ being the maximal frequency value of the frequency band $[0, \bar{\omega}]$. The computation of the \mathcal{H}_- index over an infinite frequency range can be written as a semi-definite problem.

Lemma 2.1: *Minimum sensitivity over infinite frequency range* (Liu et al., 2005). Let $\beta > 0$ be a positive constant scalar. Then $\|\mathcal{G}_c(s)\|_{\infty}^{[0,\infty]} > \beta$, if and only if there exists a P_c such that $P_c = P_c^T$ and

$$\begin{bmatrix} A_c^T P_c + P_c A_c + C_c^T C_c & P_c B_c + C_c^T D \\ B_c^T P_c + D^T C_c & D^T D - \beta^2 I \end{bmatrix} \succ 0. \quad (7)$$

Proof: The proof can be found in Liu et al. (2005). ■

Note that (7) is a linear matrix inequality (LMI), where $\succ 0$ refers to positive definiteness, therefore Lemma 2.1 can be seen either as a feasibility test (fixed value of β) or as a semi-definite optimisation problem (β is a variable) subject to LMI constraints.

It is obvious, that for strictly proper systems (i.e. $D = 0$) the above definition and formulation yields zero. In order to overcome this problem and compute the minimum sensitivity over a limited frequency interval, Liu et al. (2005) proposed the use of specific frequency filters to augment the plant. Then an estimation can be given on the frequency limited \mathcal{H}_- index of the strictly proper system. This approach has been also used by the authors in their previous work (Baár & Luspay, 2019)¹.

In order to avoid the introduction of frequency filters, a finite frequency extension from the work of Wang and Yang (2008) is used through the paper. This formulation is based on the Generalised GKYP lemma (introduced by Iwasaki et al. (2000)) and states that over a finite frequency range, the minimum sensitivity can be calculated for strictly proper systems by the following lemma.

Lemma 2.2: *Minimum sensitivity over finite frequency range* (Wang & Yang, 2008). Consider the system given in (1) with transfer function matrix (4). Let $\Pi = \begin{bmatrix} -I & 0 \\ 0 & \beta^2 I \end{bmatrix} \in \mathbb{R}^{(n_x+n_y) \times (n_x+n_y)}$ and $\underline{\omega}, \bar{\omega}$ denote the minimum and maximum frequencies, respectively, in the interested frequency range, with $\bar{\omega} = \frac{\underline{\omega} + \bar{\omega}}{2}$. Then $\|\mathcal{G}_c(s)\|_{\infty}^{[\underline{\omega}, \bar{\omega}]} > \beta$ if and only if there exists hermitian P_c and Q_c , with $Q_c \succ 0$ satisfying

$$\begin{bmatrix} A_c & B_c \\ I & 0 \end{bmatrix}^T \Xi \begin{bmatrix} A_c & B_c \\ I & 0 \end{bmatrix} + \begin{bmatrix} C_c & D \\ 0 & I \end{bmatrix}^T \Pi \begin{bmatrix} C_c & D \\ 0 & I \end{bmatrix} \prec 0, \quad (8)$$

$$\text{where } \Xi = \begin{bmatrix} -Q_c & P_c + j\frac{\bar{\omega}}{2} Q_c \\ P_c - j\frac{\bar{\omega}}{2} Q_c & -\underline{\omega}\bar{\omega} Q_c \end{bmatrix}.$$

Proof: The proof is available in Wang and Yang (2008) and omitted here. ■

Note that (7) is a special case of (8), and with the selection of $Q_c = 0$, (8) reduces to (7). Since the \mathcal{H}_- index denotes the smallest singular value, the above-mentioned formulations are also applicable to unstable systems without any modifications. However, there is a restriction for the application of the concept of \mathcal{H}_- index. Li and Liu (2010) has already raised that this index can only be calculated for tall and square systems. Nevertheless, involving the dual representation, the following lemma can be stated.

Lemma 2.3: *Calculation constraints of the minimum sensitivity index.* The \mathcal{H}_- index with the LMI formulations given in (7) and (8) can only be calculated for tall and square systems. For wide systems, the dual representation provides the appropriate \mathcal{H}_- index value.

Proof: No formal proof of this property was found by the authors, however, we believe that it is useful and helpful for understanding the developed results, therefore the derivation is reported in Appendix 1. ■

2.4 Maximum sensitivity

The well-known \mathcal{H}_∞ norm is used in the paper for characterising the maximum sensitivity of the $\mathcal{G}_d(s)$ transfer function, corresponding to the subsystem to be decoupled. The worst case gain of the system is defined as

$$\|\mathcal{G}_d(s)\|_{\infty} := \sup_{\omega} \bar{\sigma}[\mathcal{G}_d(j\omega)], \quad (9)$$

where $\bar{\sigma}$ denotes the maximum singular value. Again we are using an LMI-based computation of the \mathcal{H}_∞ norm over the $[0, \infty)$ frequency range given by the Bounded Real Lemma, which is summarised in Lemma 2.4.

Lemma 2.4: *The Bounded Real Lemma* (Scherer & Weiland, 2000). Let $\gamma \geq 0$ be a positive constant scalar. Then $\|\mathcal{G}_d(s)\|_{\infty}^{[0,\infty)} < \gamma$ if and only if there exists a positive definite symmetric $P_d = P_d^T \succ 0$, such that

$$\begin{bmatrix} A_d^T P_d + P_d A_d + C_d^T C_d & P_d B_d + C_d^T D \\ B_d^T P_d + D^T C_d & D^T D - \gamma^2 I \end{bmatrix} \preceq 0. \quad (10)$$

Proof: The proof can be found in most of the robust control textbooks, see e.g. Scherer and Weiland (2000). ■

The \mathcal{H}_∞ norm is defined only for stable systems (i.e. poles having negative real part). At the same time, unstable systems that have no poles on the imaginary axis have an \mathcal{L}_∞ norm (also known as the peak gain). This peak gain can be computed using (10) after mirroring the unstable poles over the imaginary axis (Zhou & Doyle, 1998). This modification is used in the decoupling algorithm for the case of unstable modes.

3. Problem formulation

With having defined the minimum and maximum sensitivities, we are in the position to formalise the underlying problem.

Based on Figure 1, the problem can be stated as follows. Create the environment denoted by the dashed frame, which makes possible the control of the subsystem $\mathcal{G}_c(s)$ by a corresponding controller $\mathcal{C}_c(s)$, without having the least effect on subsystem $\mathcal{G}_d(s)$. This is formalised in the paper as the minimum sensitivity from \bar{u} to \bar{y} through $\mathcal{G}_c(s)$ is maximised, while the maximum sensitivity through $\mathcal{G}_d(s)$ is minimised.

This is achieved by appropriately blending the input and output vectors of the system. For this purpose, we introduce $k_u \in \mathbb{R}^{n_u \times 1}$ and $k_y \in \mathbb{R}^{n_y \times 1}$: the normalised (i.e. $\|k_u\| = \|k_y\| = 1$)

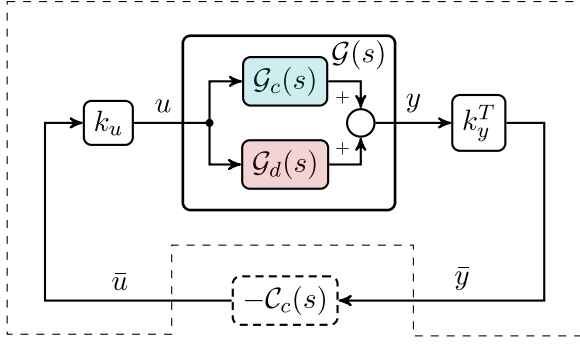


Figure 1. Closed loop control scheme with input and output blending.

input and output blending vectors, respectively. These blending vectors transform the signal vectors u and y onto a single dimension, consequently reducing the control problem into a SISO one. In Figure 1, the control input $\bar{u} \in \mathbb{R}$ is distributed between the plant's inputs ($u = k_u \bar{u}$) in a way that they only excite the subsystem which one wishes to control. Similarly the controller's input $\bar{y} = k_y^T y \in \mathbb{R}$ is calculated such that the information content from the subsystem which has to be decoupled, is minimised. We summarise the blending problem as follows.

Problem 3.1: *The decoupling problem. Find normalised vectors k_u and k_y such that*

$$\|k_y^T \mathcal{G}_c(s) k_u\|_{-}^{[\underline{\omega}, \bar{\omega}]} > \beta \quad (11)$$

is maximised, while

$$\|k_y^T \mathcal{G}_d(s) k_u\|_{\infty} < \gamma \quad (12)$$

is minimised over the selected frequency range $[\underline{\omega}, \bar{\omega}]$. Here β and γ are two positive constants referring to the minimal sensitivity and peak norm, respectively.

4. The proposed decoupling algorithm

The decoupling approach presented in the paper is carried out in two consecutive steps. First an optimal input blend is found and applied to the system, next a corresponding output blend is calculated.

4.1 Input blend calculation

The aim of the section is to find an input blend vector k_u , which maximises the excitation of the selected mode, while minimises the impact on the one(s) to be decoupled. In this step, only the state dynamics are considered, and the measurement equations are removed from the model equations.

The concept is shown in Figure 2. Here \bar{u} is the scalar input from the SISO controller $C_c(s)$ (see Figure 1), k_u is an n_u dimensional column vector distributing the blended input to the real input channels. Using our terminology the decoupling is formulated as: the sensitivity (\mathcal{H}_- index) from \bar{u} to the performance output y_c is to be maximised, while the worst case gain (\mathcal{H}_∞ norm) from \bar{u} to y_d is minimised.

Before going into the details, we mention that the input blend calculation uses the dual representation (see Section 2.2). This

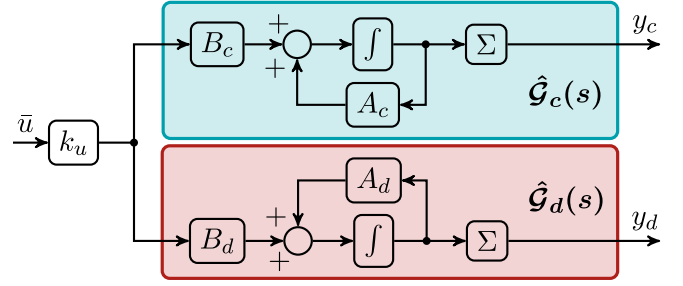


Figure 2. Problem layout for input blend calculation.

is a necessary step to keep the optimisation problem linear in the variables, as explained later. At the same time, we refer to Lemma 2.3: the \mathcal{H}_- index can only be calculated for tall or square systems. Therefore, in case the inputs are blended into a scalar signal \bar{u} , then the dual representation would be a wide system. The problem is then converted to a square system, by defining the performance output as the sum of the states as it is shown in Figure 2.

Accordingly, if one writes the LMIs (8) and (10) for the dual system and then expresses the formulas in terms of the original representation, one gets the following²

$$\begin{bmatrix} A_c^T & C_c^T \\ I & 0 \end{bmatrix}^T \Xi \begin{bmatrix} A_c^T & C_c^T \\ I & 0 \end{bmatrix} + \begin{bmatrix} B_c^T & D^T \\ 0 & I \end{bmatrix}^T \Pi \begin{bmatrix} B_c^T & D^T \\ 0 & I \end{bmatrix} < 0, \quad (13)$$

and

$$\begin{bmatrix} P_d A_d^T + A_d P_d + B_d K_u B_d^T & P_d C_d^T + B_d K_u D^T \\ C_d P_d + D K_u B_d^T & D K_u D^T - \gamma^2 I \end{bmatrix} \leq 0, \quad (14)$$

where $\Pi = \begin{bmatrix} -K_u & 0 \\ 0 & \beta^2 I \end{bmatrix}$. Here we have introduced the new matrix variable $K_u = k_u k_u^T \in \mathbb{R}^{n_u \times n_u}$, as the dyadic product of the input blend vector.

It should be clear that the terms involving K_u are appearing in the LMIs only because of the dual representation, otherwise we would be facing a bilinear (and quadratic) matrix problem, i.e. the dual form ensures linearity. Nevertheless, the newly introduced variable K_u is a rank 1 matrix, which has to be taken into consideration in the solution. The input blend calculation is summarised in Proposition 4.1.

Proposition 4.1: *The input blend design. The optimal input blend k_u for the system given in the form of (1) can be calculated as the left singular vector corresponding to the largest singular value of the blend matrix K_u , where K_u satisfies the following optimisation problem*

$$\begin{aligned} & \text{minimise} && -\beta^2 + \gamma^2 \\ & P_d, K_u, P_c, Q, \beta^2, \gamma^2 \\ & \text{subject to} && (13), (14), P_d = P_d^T, P_d \geq 0, \\ & && P_c = P_c^T, Q = Q^T, Q \geq 0, \\ & && 0 \leq K_u \leq I, \quad \text{and} \quad \text{rank}(K_u) = 1, \end{aligned} \quad (15)$$

with I being the identity matrix with appropriate dimensions.

Proposition 4.1 is a multi-objective optimisation problem, which is frequent in mixed $\mathcal{H}_-/\mathcal{H}_\infty$ fault detection observer

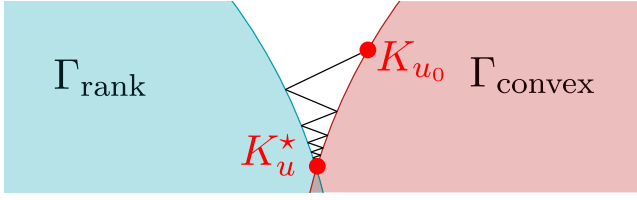


Figure 3. Alternating projections.

design (see e.g. Wang et al., 2007). However, concerning the rank constraint, some further remarks are required. The rank(K_u) = 1 constraint in an earlier version of the algorithm has been satisfied by a rank minimisation heuristic. In practice, this means the incorporation of the term $\text{trace}(K_u)$ in the objective function of (15). For further details see Baár and Luspay (2019). However, this approach does not guarantee the satisfaction of the rank constraint and was found to be numerically sensitive.

Therefore, in the present paper, we wish to take one step further and apply a more systematic approach for the solution of Proposition 4.1. More precisely, we use an alternating projection scheme to ensure the rank-1 constraint of the blending matrix K_u .

The main idea was taken and tailored from Grigoriadis and Beran (2000), where the authors used an alternating projection technique for satisfying a coupling rank constraint in a fixed-order \mathcal{H}_∞ control design problem. For the solution of the present problem, the basic idea is the following. Introduce the convex set Γ_{convex} which is described by the LMIs (13) and (14) without the rank constraint on the blend matrix K_u . Denote this non-convex rank constraint on K_u by the set Γ_{rank} . Suppose that the sets have a nonempty intersection, and one wishes to solve the problem by finding a matrix in the intersection. The alternating projection scheme tells us that this problem can be solved by a sequence of orthogonal projections from one set to the other. Each step assures that the projected matrix in the corresponding set has the smallest distance from the one which was projected. The orthogonal projection theorem also assures that each projection is unique (Luenberger, 1997). However, even if the intersection exists, global convergence cannot be guaranteed in our case, due to the non-convex set Γ_{rank} . Nevertheless local convergence of the proposed algorithm to a matrix which satisfies the above constraints is guaranteed (Grigoriadis & Beran, 2000).

The approach consists of various sequences of alternating projections. In each sequence the dimension of the set Γ_{rank} is reduced by one (starting from n_u , until $\text{rank}(K_u^*) = 1$ is achieved. The process of a single projection sequence is illustrated in Figure 3. Next the solution of Proposition 4.1 based on an alternating projection algorithm is presented in details. For this we apply the following two lemmas.

Lemma 4.2: *Orthogonal projection to a lower dimensional set (Grigoriadis & Beran, 2000). Let $Z \in \Gamma_{\text{rank}}^{n \times n}$ and let $Z = USV^T$ be a singular value decomposition of Z . The orthogonal projection, $Z^* = \mathcal{P}_{\Gamma_{\text{rank}}^{n-k}} Z$, of Z onto the $\Gamma_{\text{rank}}^{n-k \times n-k}$ dimensional set is given by*

$$Z^* = US_{n-k}V^T, \quad (16)$$

where the S_{n-k} diagonal matrix is obtained by replacing the smallest k singular values by zeros.

Lemma 4.3: *Projection to a general LMI constraint set Γ (Grigoriadis & Beran, 2000). Let Γ be a convex set, described by an LMI. Then the projection $X^* = P_\Gamma X$ can be computed as the unique solution Y to the semi-definite programming problem*

$$\begin{aligned} & \text{minimise } \text{trace}(S) \\ & \text{subject to } \begin{bmatrix} S & Y - X \\ Y - X & I \end{bmatrix} \geq 0, \\ & Y \in \Gamma, \quad S, Y, X \in R^{n \times n}, \end{aligned} \quad (17)$$

with $S = S^T$.

Proof: For further details about the alternating projection method, the reader is invited to consult with Grigoriadis and Beran (2000). ■

Now we are in the position to present the proposed solution to Proposition 4.1. The process is summarised in Algorithm 1, which can be found in Appendix 2. Each of its steps are discussed next.

The solution process starts with defining the subsystem one wishes to control and the subsystem one wishes to decouple from it, where the systems are transformed to the form as shown in Figure 2. This is the starting point of Algorithm 1, in line 1.

Next the optimisation problem presented in Proposition 4.1 is solved, without the arising rank constraint. The blend matrix is constrained to be symmetric and $0 \leq K_u \leq I$. According to Grigoriadis and Beran (2000), a term $\text{trace}(K_u)$ is added to the objective function for forcing the blend matrix K_u towards a lower rank solution. This provides K_{u_0} which is the initial value in the following alternating projection sequences. The corresponding step is given in line 2 of Algorithm 1 and provides the achievable values for β and γ .

The alternating projection scheme starts at line 3, where the computed β and γ are kept constant. In each of the outer loops the dimension of the rank constraint set is reduced by one, while the inner loop contains the alternating projection to obtain the corresponding reduced rank solution. Once the solution is obtained by fulfilling the stopping criteria, the outer loop reduces the rank further, until 1 is achieved.

The blend vector k_u can be found from the singular value decomposition of the blend matrix K_u^* , upon the convergence: it is the left singular vector corresponding to the largest singular value of K_u^* . Once k_u is found, it is applied to the subsystems to give

$$\begin{aligned} \dot{x}_{\{c,d\}}(t) &= A_{\{c,d\}}x_{\{c,d\}}(t) + B_{\{c,d\}}k_u\bar{u}(t), \\ y_{\{c,d\}}(t) &= C_{\{c,d\}}x_{\{c,d\}}(t) + Dk_u\bar{u}(t). \end{aligned} \quad (18)$$

In the following we use the notation $\bar{A}_{\{c,d\}} = A_{\{c,d\}}$, $\bar{B}_{\{c,d\}} = B_{\{c,d\}}k_u$, $\bar{C}_{\{c,d\}} = C_{\{c,d\}}$, $\bar{D} = Dk_u$ for the input-blended representation and discuss the corresponding output blend computation.

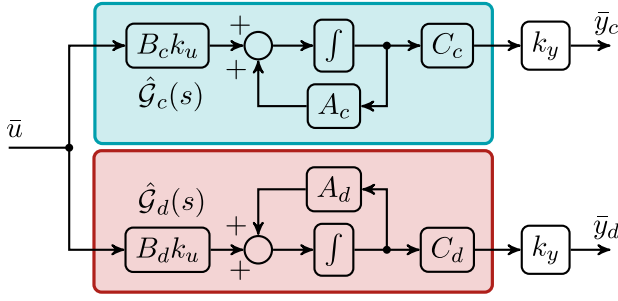


Figure 4. Problem layout for output blend calculation.

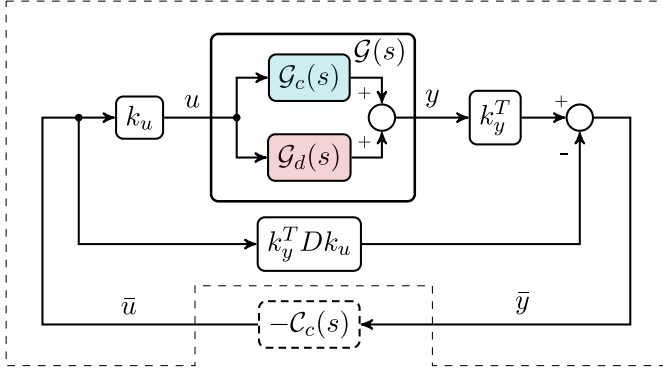


Figure 5. Closed loop control scheme with input and output blending.

4.2 Output blend calculation

The aim of this section is to find a linear combination of the available outputs such that the desired subsystem is observed as much as possible, while the other one appears as less as possible in the blended measurement. Using the introduced terms, k_y^T should create a single blended output, with having maximal sensitivity on the performance output of the subsystem to be controlled, and minimal transfer on the one to be decoupled. The approach is similar to the input blend calculation. The process is summarised in Figure 4. The direct feedthrough term from the given inputs to the outputs is the same for both modes, and it was already neglected at the input blend calculation. For this reason, we propose to remove the term D from both of the systems and calculate the output blend without it. In the closed loop control, the effect of the direct feedthrough can be taken into account as shown in Figure 5. Only for the completeness of the inequalities, the terms D are retained in the following equations.

The necessary LMI constraints for the optimisation problem concerning the subsystem to be controlled and to be decoupled are given by

$$\begin{bmatrix} \bar{A}_c & \bar{B}_c \\ I & 0 \end{bmatrix}^T \Xi \begin{bmatrix} \bar{A}_c & \bar{B}_c \\ I & 0 \end{bmatrix} + \begin{bmatrix} \bar{C}_c & \bar{D}_c \\ 0 & I \end{bmatrix}^T \Pi \begin{bmatrix} \bar{C}_c & \bar{D}_c \\ 0 & I \end{bmatrix} < 0, \quad (19)$$

and

$$\begin{bmatrix} \bar{A}_d^T P_d + P_d \bar{A}_d + \bar{C}_d^T K_y \bar{C}_d & P_d \bar{B}_d + \bar{C}_d^T K_y \bar{D}_d \\ \bar{B}_d^T P_d + \bar{D}_d^T K_y \bar{C}_d & \bar{D}_d^T K_y \bar{D}_d - \gamma^2 I \end{bmatrix} \leq 0, \quad (20)$$

respectively, where $\Pi = \begin{bmatrix} -K_y & 0 \\ 0 & \beta^2 I \end{bmatrix}$. Here we introduced the output blend matrix $K_y = k_y k_y^T$. The optimisation problem to

be solved is given in Proposition 4.4 with variables P_c , Q , P_d , K_y , β^2 , γ^2 .

Proposition 4.4: *The output blend design. The optimal output blend vector k_y for the system given in (18) can be calculated as the left singular vector corresponding to the largest singular value of the blend matrix K_y , where K_y satisfies the following optimisation problem*

$$\begin{aligned} & \underset{P_d, K_y, P_c, Q, \beta^2, \gamma^2}{\text{minimise}} && -\beta^2 + \gamma^2 \\ & \text{subject to (19), (20), } && P_d = P_d^T, P_d \geq 0, \\ & && P_c = P_c^T Q = Q^T, Q \geq 0, \\ & && K_y = K_y^T, 0 \leq K_y \leq I, \text{ and } \text{rank}(K_y) = 1. \end{aligned} \quad (21)$$

The rank one solution for the blend matrix K_y can be achieved by a similar alternating projection algorithm as in the case of the input blend. This is summarised in Algorithm 2, which can be found in Appendix 3.

By applying the output blend to each of the subsystems, they will have the form

$$\begin{aligned} \dot{x}_{\{c,d\}}(t) &= A_{\{c,d\}} x_{\{c,d\}}(t) + B_{\{c,d\}} k_u \bar{u}(t), \\ \bar{y}_{\{c,d\}}(t) &= k_y^T C_{\{c,d\}} x_{\{c,d\}}(t) + k_y^T D k_u \bar{u}(t). \end{aligned} \quad (22)$$

Note that the direct feedthrough term was not involved into the optimisation process which means that the optimal transformation of D by the blend vectors k_u and k_y^T is not guaranteed. However, since the D term is the same for each modes, it is possible to modify the overall control scheme presented in Figure 1, by introducing a feedforward term $k_y^T D k_u$, as shown in Figure 5.

Remark 4.1: It might be desirable to identify some metrics which provide information about whether the decoupling is possible before calculating the actual blend vectors. According to Hamdan and Nayfeh (1989), the magnitude of $|q_i^T b_j| = |q_i| |b_j| \cos(\theta_{ij})$ is an indication of controllability of the i^{th} mode from the j^{th} input, where q_i is the left eigenvector corresponding to the i^{th} mode, b_j is the input vector corresponding to the j^{th} input, and $\cos(\theta_{ij})$ is the angle between the two vectors. In the applied modal form, this reduces to the following criteria for the i^{th} mode. In order to be controllable from the j^{th} input, the input vector b_j should contain non-zero elements in the rows corresponding to the i^{th} mode. The magnitude of these elements are measures of controllability. In case of the blend calculation problem, this means that the blended input matrix $B k_u$ should contain non-zero values at the locations corresponding to the targeted mode, while it's other elements should be small, possibly zero. This is clearly achievable if the row vectors of B_d are far from the subspace spanned by the rows of B_c . Similar reasoning corresponds to the output decoupling, based on observability and the columns of C . However the detailed investigation of these decoupling criteria are out of the paper's scope and will be investigated in the future.

Remark 4.2: Based on our experience, the order of the blend calculation can be changed. It is possible to calculate an output blending vector first and then find a corresponding input blend.

The resulting vector elements can slightly differ for the two sequences, however, the directions are the same in both cases. The similar can be said about the comparison of the results with other blending approaches (such as Pusch, 2018): although the formulations and the obtained blend vectors are numerically different, the directions are nearly the same.

4.3 The decoupling of multiple modes

Throughout the paper, we have supposed that the $\{\cdot\}_c$ subsystem consists of only one mode. In the following, we show that this limitation can be relaxed with some minor modifications. Accordingly, we present two possible extension of the algorithm, which can assure the decoupling of multiple modes.

4.3.1 SISO decoupling

We call this method SISO decoupling because all the targeted modes are controlled with the same SISO controller. Necessary requirements towards the blend vectors are that they decouple the subsystems $\{\cdot\}_c$ and $\{\cdot\}_d$, while preserving controllability and observability of the targeted modes. For the ease of presentation we assume that the subsystem $\{\cdot\}_c$ consists of two subsystems and has the form

$$\begin{aligned} A_c &= \begin{bmatrix} A_{c_1} & 0 \\ 0 & A_{c_2} \end{bmatrix}, & B_c &= \begin{bmatrix} B_{c_1} \\ B_{c_2} \end{bmatrix}, \\ C_c &= [C_{c_1} \quad C_{c_2}], & D &= [D]. \end{aligned} \quad (23)$$

In case of input decoupling the first issue that one has to tackle is to assure that both of the blended subsystems remain controllable separately. According to Remark 4.1, the measure of controllability of each of the modes from the j^{th} input is proportional to the magnitude of the j^{th} column vectors in B_{c_1} and B_{c_2} respectively. From this it follows that in order to keep both of the modes controllable a necessary requirement is that the blended inputs $B_{c_1}k_u$ and $B_{c_2}k_u$, respectively, should not be zero vectors. It can be assured by adding further constraints to Proposition 4.1 as

$$\text{trace}(B_{c_1}K_u B_{c_1}^T) \geq b_{1\min} \quad \text{and} \quad \text{trace}(B_{c_2}K_u B_{c_2}^T) \geq b_{2\min}. \quad (24)$$

The terms $b_{1\min}$ and $b_{2\min}$ are tuneable parameters, reflecting the level of controllability of each of the modes. Once they are set to a low value, the algorithm may find a blend vector which assures higher suppression of the undesired dynamics, on the expense of larger control input energy to control the targeted subsystem.

Once the subsystems are separately controllable, one has to show that they can be controlled by the same blended input. This can be done by the Popov–Belevitch–Hautus (PBH) controllability test (Kailath, 1980). It states that the system is controllable when

$$\text{rank} \left(\begin{bmatrix} sI - A_{c_1} & 0 & B_{c_1}k_u \\ 0 & sI - A_{c_2} & B_{c_2}k_u \end{bmatrix} \right) = \dim(A_c), \quad (25)$$

where $s \in \mathbb{C}$. It is obvious that rank deficiency can only arise when s equals to one of the eigenvalues of the subblocks A_{c_i} , otherwise full rank is guaranteed. At the same time, condition (24) ensures full rank of the extended matrix at the poles

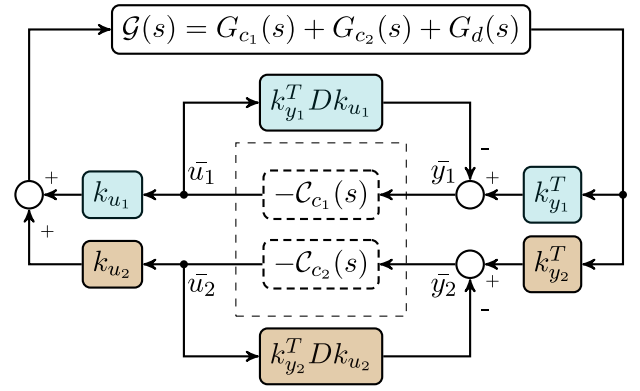


Figure 6. Closed loop control scheme for the MIMO decoupling approach.

of the subsystems, except to the particular case of $A_{c_1} = A_{c_2}$. This is not surprising, since two identical subsystems cannot be controlled by a single input. Consequently, this condition is the main limitation of the proposed blending approach, when applied for higher dimensional subsystems, instead of single modes. Observability properties can be shown in a similar way.

4.3.2 MIMO decoupling

When the subsystem to be controlled consists of multiple modes, it is also possible to convert the problem into a MIMO one, and control each of the modes with a corresponding SISO controller. This case is shown in Figure 6, where we have supposed that the subsystem to be controlled consists of two modes. The dashed frame denotes the interface between the blended system and the SISO controllers. The blend vectors k_{u_1} and $k_{y_1}^T$ are designed in a way that they suppress the effects of $G_{c_2}(s)$ and $G_d(s)$. The same method applies to k_{u_2} and $k_{y_2}^T$. Note that the diagonalisation of the two input two output system is only possible, when the input and output null spaces of $G_1(s) = G_{c_1}(s) + G_d(s)$ and $G_2(s) = G_{c_2}(s) + G_d(s)$ exists. Otherwise the resulting transfer function matrix is not guaranteed to be diagonally dominant. Additional approaches to suppress the offdiagonal elements should be investigated in the future, such as the method of decoupling by feedback (Wang, 2002).

5. Numerical examples

Before turning our attention towards the numerical evaluation of the proposed decoupling algorithm, it is worth to examine the theoretically achievable best solutions.

First consider the maximisation of the minimal sensitivity for the transfer corresponding to the controlled subsystem. The decoupling is carried out by one-norm blend vectors k_u and k_y^T . By applying matrix norm identities on an arbitrary transfer function matrix $\mathcal{G}_{n_y \times n_u}$, one gets:

$$\frac{1}{\sqrt{n_u}} \|\mathcal{G}\|_{i\infty} \leq \bar{\sigma}(\mathcal{G}), \quad (26)$$

where $\|\cdot\|_{i\infty}$ is the maximal row sum. This shows that with a normalised blending, the maximum achievable singular value is bounded from above. Consequently by applying one-norm input and output blends, no higher \mathcal{H}_- index can be achieved than the maximum singular value of the given subsystem.

Concerning the suppression of the subsystem to be decoupled, the highest suppression rate can be achieved if the blended inputs or outputs are as close as possible to the corresponding null spaces. A blending approach proposed by Pusch (2018) carries out decoupling based on a null space transformation. This approach is certainly valid, however, the existence of null space and its sensitivity for model parameters and changes might hinder its application for real problems.

All the following examples were created by using YALMIP (see Löfberg, 2004) in the Matlab environment, with the SeDuMi solver (Sturm, 1999).

5.1 Academic example

First we evaluate the proposed method based on a simple academic example, in order to make the results reproducible for the reader. The example is given by

$$\begin{aligned} A &= \begin{bmatrix} A_c & 0 \\ 0 & A_d \end{bmatrix} = \begin{bmatrix} -0.4 & 1.6 & 0 \\ -1.6 & -0.4 & 0 \\ 0 & 0 & -1.4 \end{bmatrix}, \\ B &= \begin{bmatrix} B_c \\ B_d \end{bmatrix} = \begin{bmatrix} 0.7 & -0.1 & 0.3 \\ -0.4 & -0.2 & 0.1 \\ -0.6 & -0.2 & 0.8 \end{bmatrix}, \\ C &= [C_c \quad C_d] = \begin{bmatrix} 0 & 0.8 & -0.8 \\ -0.8 & -0.7 & -0.9 \end{bmatrix}, \quad D = 0. \end{aligned} \quad (27)$$

The system consists of two stable modes, where we wish to control the first complex one, and decouple from it the real one. The controllability and observability properties of the modes can be quantified by the eigenvalues of their controllability and observability Gramians. The controllability Gramian denoted by W is calculated as the positive definite solution of the following Lyapunov equation:

$$AW + WA^T + BB^T = 0. \quad (28)$$

The needed control energy by the system is proportional by the inverse of the Gramian. In the present example, the Gramians corresponding to the subsystems $\{\cdot\}_c$ and $\{\cdot\}_d$, have the eigenvalues

$$\lambda_c(W_c) = [0.4096 \quad 0.5904], \quad \text{and} \quad \lambda_d(W_d) = 0.3714. \quad (29)$$

The observability Gramian V is similarly defined as the positive definite solution of

$$A^T V + VA + C^T C = 0. \quad (30)$$

Its eigenvalues are proportional to the observation energy of the system. For the given subsystems the observability Gramians have eigenvalues as

$$\lambda_c(V) = [0.9209 \quad 1.2916], \quad \lambda_d(V) = 0.5179. \quad (31)$$

The blend vectors k_u and k_y are calculated based on Section 4. The frequency interval where the decoupling should be achieved was selected to be between 0 and $\omega_n \frac{\text{rad}}{\text{s}}$, where the latter stands for the natural frequency of the mode to be controlled, i.e. in (8) $\underline{\omega} = 0$ and $\bar{\omega} = \omega_n$. The blend

vectors are $k_u^T = [-0.7979 \quad -0.0167 \quad -0.6026]^T$ and $k_y^T = [-0.6956 \quad 0.7185]^T$ respectively. Figure 7 shows the maximum singular values of the subsystems, which are corresponding to the highest achievable sensitivity by suitable blends according to (26). Note that the subsystem corresponding to the undesired dynamics has higher steady state gain than the one to be controlled. As the lower subfigure shows after applying the input and output blends, this theoretically maximal sensitivity was retained, while the transfer through the other (undesired) mode was significantly reduced.

Of course the decoupling has its own price, which can be revealed by calculating the eigenvalues of the controllability and observability Gramians corresponding to the blended subsystems. These are found to be

$$\begin{aligned} \lambda_c(\tilde{W}_c) &= [0.2901 \quad 0.4759], \quad \text{and} \quad \lambda_d(\tilde{W}_d) = 3.58 \cdot 10^{-14}, \\ \lambda_c(\tilde{V}_c) &= [0.6877 \quad 1.1281], \quad \text{and} \quad \lambda_d(\tilde{V}_d) = 0.0029, \end{aligned} \quad (32)$$

where $\{\tilde{\cdot}\}$ denotes that they are the Gramians corresponding to the blended subsystems. They show that an applied control action will not excite the undesired dynamical part of the system, however for this one has to sacrifice a certain amount of controllability of the mode that should be controlled. Similarly, the undesired dynamics are made unobservable, and so their effects are suppressed in the blended measurements. This can be achieved on the expense of reducing the observability of the controlled mode also.

5.2 Flexible aircraft

In the following two numerical examples from the aerospace engineering field are presented in order to validate the proposed approach. The models are taken from the FLEXOP project (2015), which aims to design and demonstrate flutter suppression techniques on a flexible winged demonstrator UAV. The demonstrator aircraft is equipped with eight ailerons (four on the left and four on the right wings) and two ruddervators on each side. Measurements are given at the 90% spanwise location on the left and right trailing edge, providing information about the vertical acceleration (a_z) and the angular rates (ω_x, ω_y) around the lateral and longitudinal axis of the aircraft respectively.

The dynamical model has the five standard aircraft rigid body modes with the additional two flutter modes arising from the coupling of aerodynamic and structural forces. The nonlinear dynamics have been trimmed and linearised over a range of admissible airspeed values, Figure 8 then shows the pole migration map of the aircraft for a simplified illustration of the dynamic modes. It can be seen that at a certain airspeed the flutter modes become unstable. For more details about the modelling and control, we refer to Luspay et al. (2018). The obtained family of linear models is then transformed into a parameter varying modal form and a parameter varying model order reduction was performed (Luspay et al., 2018). The obtained low order model is given in its modal form and used for illustrating the proposed decoupling methodology.

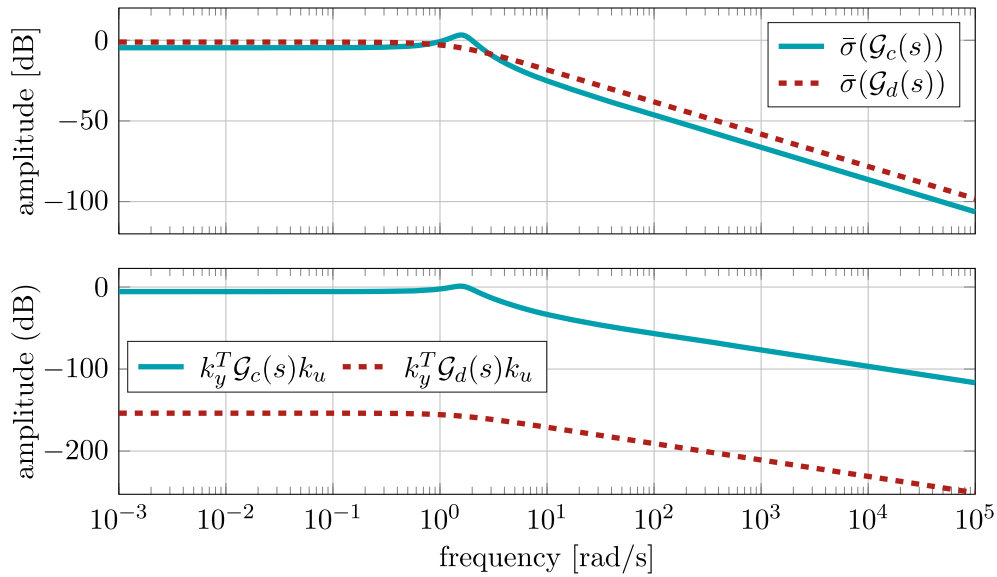


Figure 7. Above: The maximum singular values of the subsystems before blending. Below: The singular values of the blended SISO subsystems.

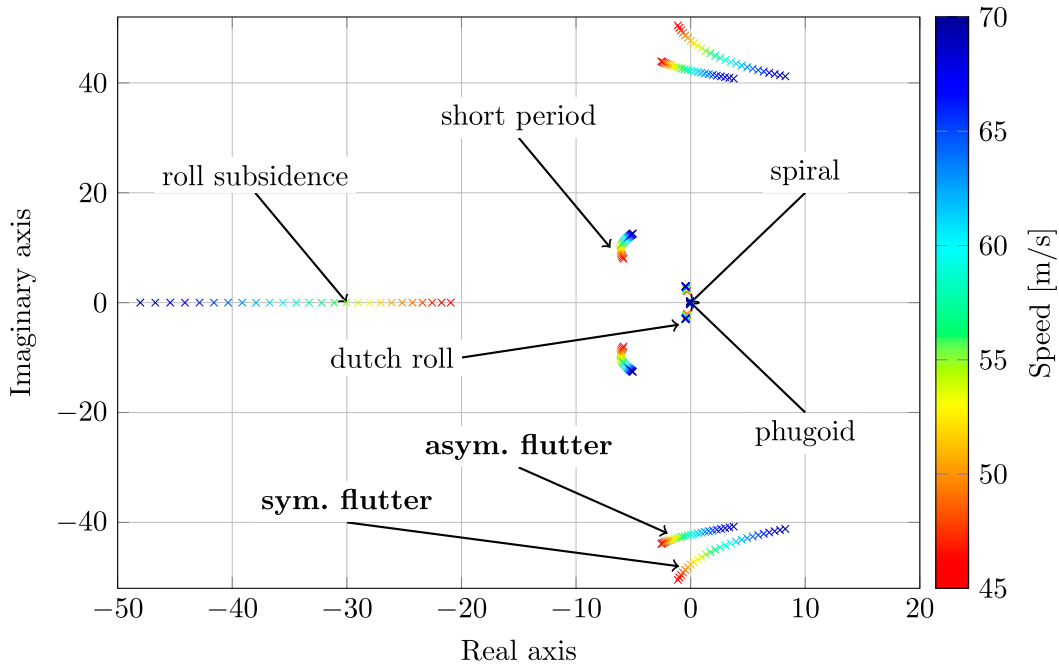


Figure 8. The pole-zero map of the flexible aircraft model.

5.2.1 Decoupling of symmetric and asymmetric flutter modes

The first example involves the decoupled control of the two unstable flutter modes at the $64 \frac{\text{m}}{\text{s}}$ airspeed. The aim is to control the symmetric mode, while leaving the asymmetric one unaffected. By doing so, two separate SISO controllers can be designed for the corresponding flutter modes (Pusch et al., 2019). The frequency interval where the decoupling should be achieved was selected to be between 0 and the natural frequency of the mode to be controlled. Since the asymmetric flutter mode is unstable at the investigated airspeed, its poles were mirrored to the imaginary axis, according to the discussion in Section 2.4. The upper subfigure of Figure 9 shows the maximal singular values of the selected two flutter modes. The asymmetric mode,

which should be suppressed has higher amplifications in the $[0, 100] \frac{\text{rad}}{\text{s}}$ range. After applying the optimisation method summarised in Algorithms 1 and 2, the Bode magnitude plot of the resulting SISO subsystems without the direct feedthrough term is shown in the lower subfigure of Figure 9. Note that the sensitivity level of the mode to be controlled is slightly reduced, which is according to (26) almost the theoretical upper bound of the sensitivity. On the contrary the amplification of the asymmetric flutter mode is reduced by almost 80 dB.

5.2.2 Decoupling asymmetric flutter mode from the remaining dynamics

By the application of the proposed method, it is also possible to decouple a selected mode from the rest of the dynamics. The

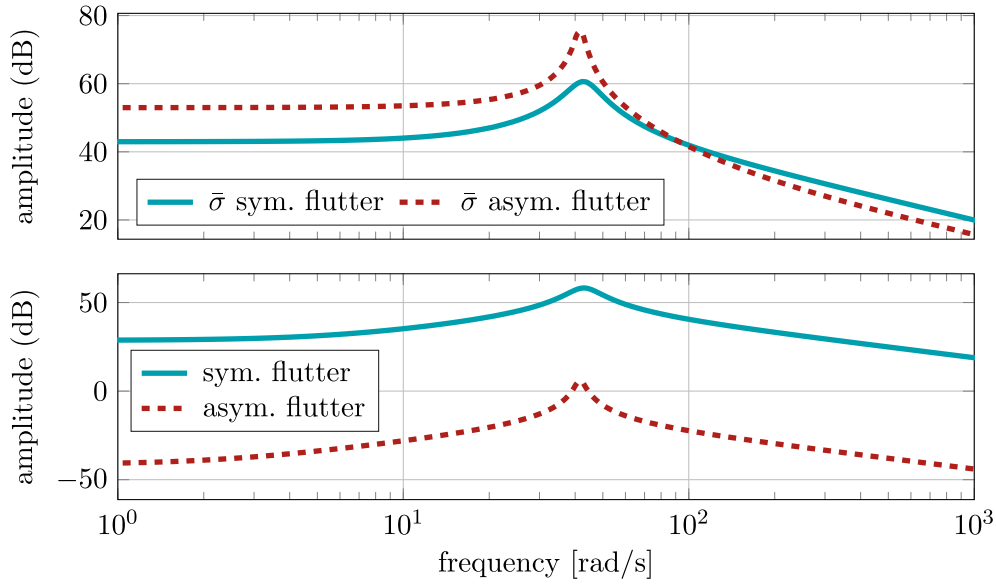


Figure 9. Above: The maximum singular values of the unstable flutter modes before blending. Below: The singular values of the blended SISO subsystems.

next example investigates this scenario for the aircraft model taken at the $47 \frac{m}{s}$ airspeed, where all the modes are stable. The aim is to effect the asymmetric flutter mode, while suppressing the rest of the dynamics including all the rigid body modes and the symmetric flutter mode.

Figure 10 shows the maximum singular values of the modes to be controlled and to be decoupled, respectively. Note that, in this example the dynamic part which should be unaffected has higher steady state gain. By applying the suitable blend vectors, the subsystems can be decoupled, in a way that almost the whole sensitivity of the controlled subsystem is retained as it is shown in the lower subfigure of Figure 10.

5.2.3 Decoupling the two flutter modes from the remaining dynamics

In this example, we investigate the case when the symmetric and asymmetric flutter modes should be controlled by a corresponding SISO controller, while the rest of the dynamics is left unattained, as described in Section 4.3.1. The aircraft model is taken at the $47 \frac{m}{s}$ airspeed. We selected $b_{i\min} = \text{trace}(B_{c_i} K_u B_{c_i}^T) / 10$ where i represents the symmetric and asymmetric flutter modes. The controllability Gramians W had the eigenvalues for the original subsystems ($\{\cdot\}_c$, and $\{\cdot\}_d$)

$$\begin{aligned} \lambda_c(W_c) &= [1.5748 \quad 1.6232 \quad 2.3507 \quad 2.6695] \cdot 10^5, \\ \lambda_d(W_d) &= [0.0072 \quad 0.0101 \quad 0.0102 \quad 0.0136 \quad 0.0192 \quad 0.1177 \quad 0.5659 \quad 1.9648] \cdot 10^4, \end{aligned} \quad (33)$$

while after the blend calculations, the Gramians for the SISO subsystems had eigenvalues

$$\begin{aligned} \lambda_c(\tilde{W}_c) &= [0.4331 \quad 0.4956 \quad 6.8686 \quad 7.1346] \cdot 10^4, \\ \lambda_d(\tilde{W}_d) &= [0.0011 \quad 0.0016 \quad 0.0053 \quad 0.0077 \quad 0.0118 \quad 0.0364 \quad 0.2856 \quad 0.3193] \cdot 10^{-3}. \end{aligned} \quad (34)$$

The singular values of the corresponding subsystems are shown in Figure 11. It was possible to decouple the two subsystems, on the expense of losing from the transfer of the targeted modes.

5.3 Batch test

In order to further evaluate the numerical properties of the decoupling methodology, a batch test was also performed.

Stable LTI models with various input ($2 \leq n_u \leq 12$) and output ($2 \leq n_y \leq 12$) dimensions were created randomly. For each IO pair 12 systems were generated with various random seeds, where each model has 4 states for the sake of simplicity. This resulted in a total number of 1452 random systems. All the LTI systems were transformed then to modal forms, and the respective first modes were selected to be controlled, and the second ones to be suppressed. Then the proposed IO blending algorithms have been run to decouple the selected modes.

We defined a suppression rate, which measures the minimum distance between the blended subsystems. The decoupling was considered successful if the suppression rate is more than 20 dB on the Bode magnitude plot, and the steady state gain for the controlled mode is higher than -20 dB. The 20 dB criteria corresponds to a minimum of ten times higher amplification of the controlled mode. Based on these criteria, the proposed algorithm achieved decoupling in 86% of the investigated test cases.

Figure 12 shows the distribution of the achieved suppression rates. Observe the two peaks in the histogram: one around 20 dB and another one around 120 dB, respectively. The first one belongs to systems which can be hardly decoupled (if at all), while the latter one to systems where higher level of decoupling was possible.

In order to further visualise the results, consider the ratio of the \mathcal{H}_- index and the \mathcal{H}_∞ norm as $\frac{\|\mathcal{G}_c(s)\|_-}{\|\mathcal{G}_d(s)\|_\infty}$. In Figure 13 this ratio is shown for each of the systems before and after of the application of the blend vectors. Red line denotes the average of

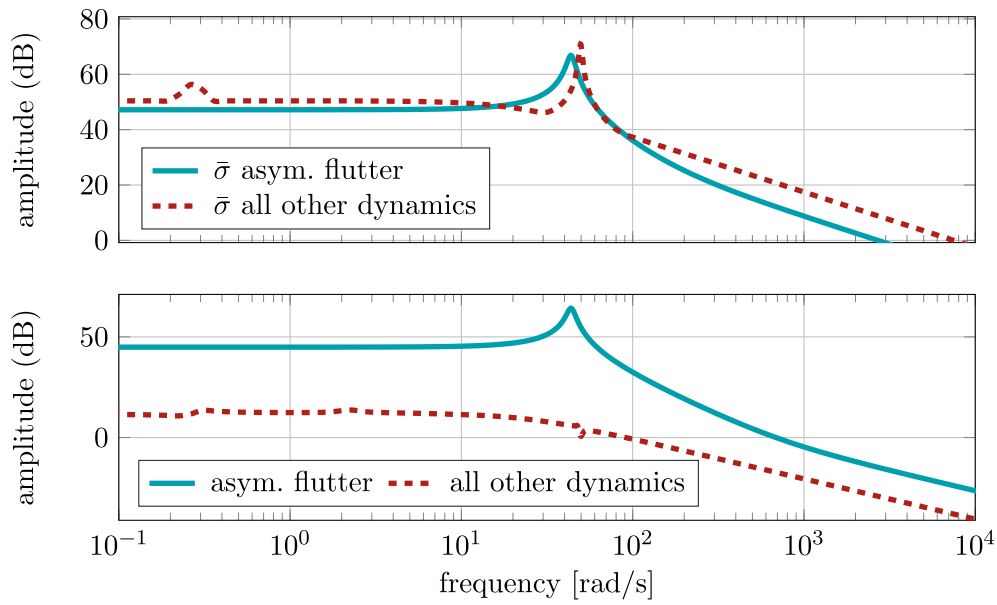


Figure 10. Above: The maximum singular values of the subsystems before blending. Below: The singular values of the blended SISO subsystems.

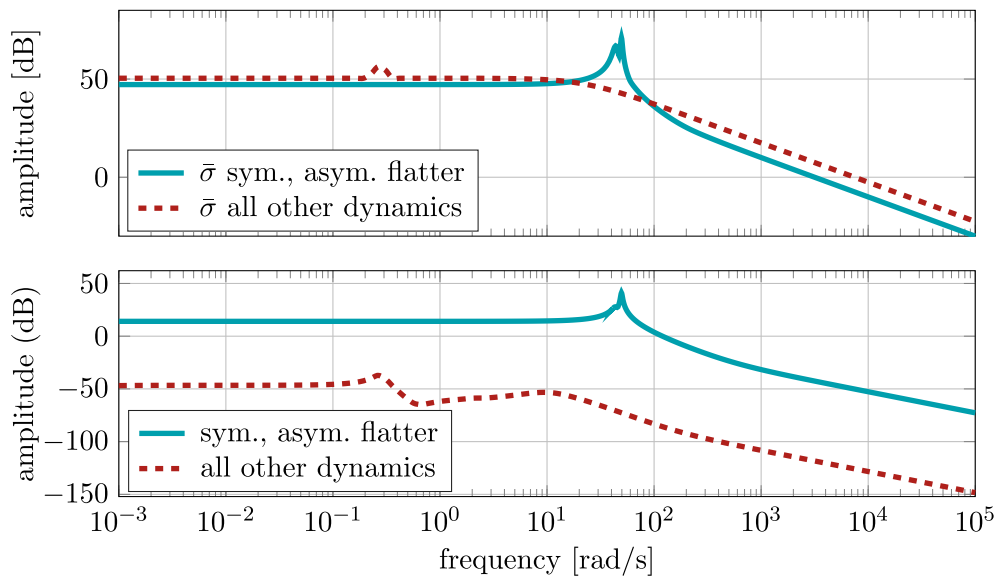


Figure 11. Above: The maximum singular values of the subsystems before blending. Below: The singular values of the blended SISO subsystems.

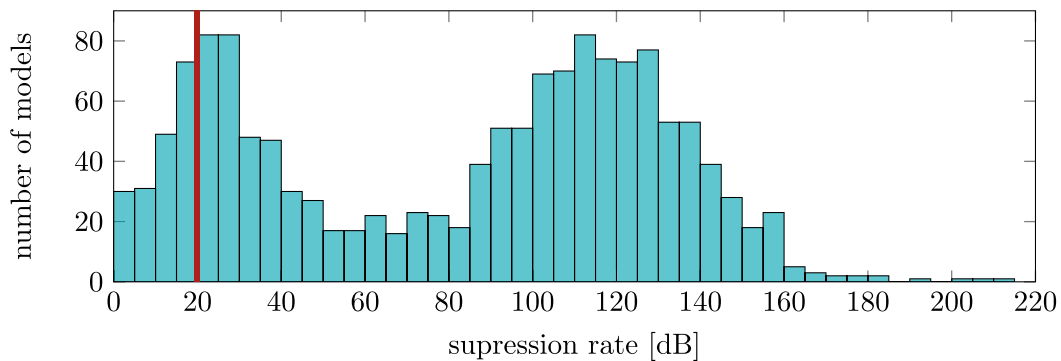


Figure 12. The distribution of the achieved suppression rates.

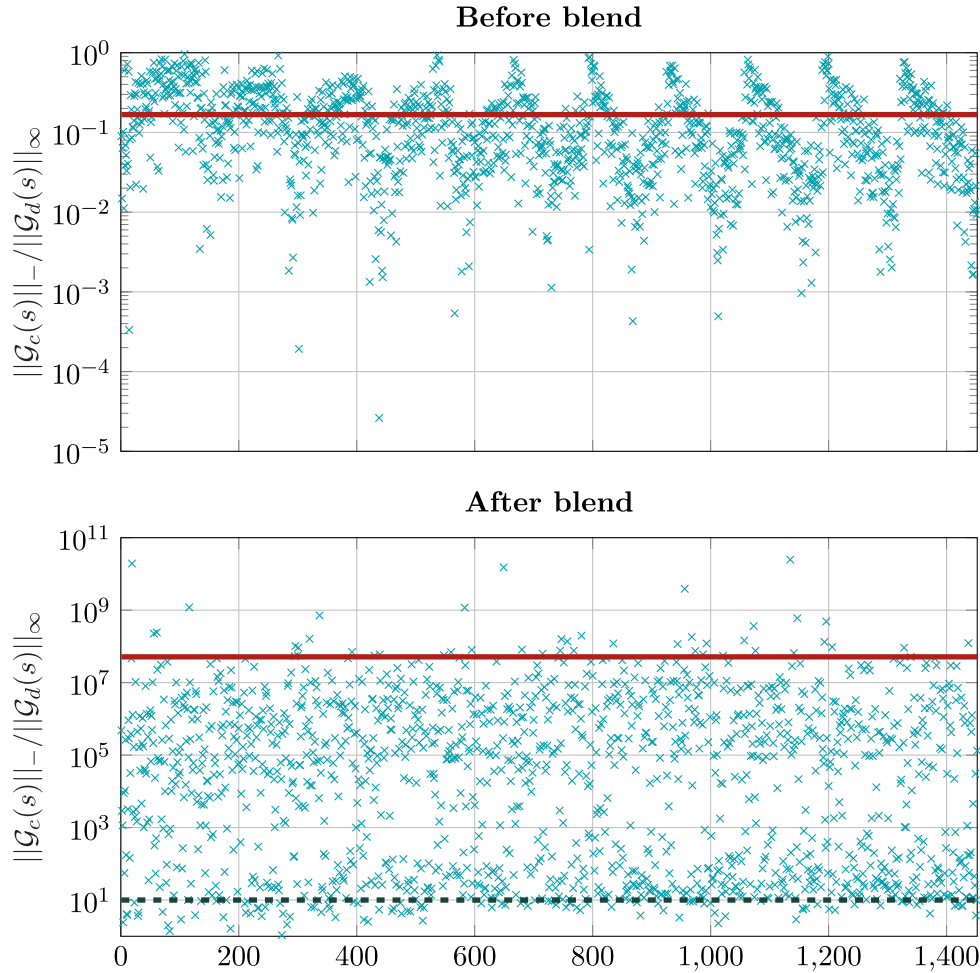


Figure 13. The $\frac{\|\mathcal{G}_c(s)\|_{\infty}}{\|\mathcal{G}_d(s)\|_{\infty}}$ ratio before and after blending for the systems in the batch test

the ratios, which is increased from 10^{-1} to 10^7 . Black dashed line represents the minimal suppression rate which has to be achieved in order to consider the decoupling successful. Only about 7% of the test cases result in a ratio below it. Due to the decoupling criteria and the 86% success rate, it also means that in 7% of the test cases the steady state gain of the controlled modes was reduced below -20 dB.

6. Conclusion

We have presented a modal decoupling approach that allows independent control of selected modes. To achieve this goal, input and output blend vectors are calculated based on a convex optimisation approach from the Robust Control literature. The proposed method has been validated based on various examples. Based on a simple academic example, it has been shown that the obtained blend vectors are maximising the controllability and observability of the targeted mode, while minimising them to the remaining subsystems. Three aerospace examples have been also reported to illustrate the decoupling in real life problems. The proposed algorithms allowed the control of the flexible motion of the wing, without having significant interaction with the rigid body dynamics. An exhausting evaluation campaign carried out over 1452 systems proved that reliable

decoupling performance is achievable by the proposed blend vectors.

The authors believe that by the use of integral quadratic constraints, the method can be extended to consider uncertain systems also. Furthermore, since the approach is based on the LMI formulation of the \mathcal{H}_{∞} index and the \mathcal{H}_{∞} norm, it is easily extendable to Linear Parameter Varying (LPV) systems. In this case the blending vector functions $k_u(\rho)$ and $k_y(\rho)$ are the results of the convex optimisation process.

Notes

1. On the other hand, our aim is to avoid the use of additional frequency filters, due to their explicit appearance and effect in the computation of the blending vectors (see Section 4).
2. The D terms are retained in the equations only for completeness; however, their value is zero during the optimisation process.

Acknowledgements

The authors would like to thank for the valuable recommendations and discussions for Bálint Patartics and György Lipták. The research leading to these results is part of the FLEXOP project.

Disclosure statement

No potential conflict of interest was reported by the author(s).

Funding



EMBERI ERŐFORRÁSOK

MINISZTERIUMA The research was supported by the ÚNKP-18-3, the ÚNKP-18-4 and the ÚNKP-19-4 New National Excellence Programs of the Ministry of Human Capacities. The research leading to these results is part of the FLEXOP project. This project has received funding from the European Unions Horizon 2020 research and innovation programme under grant agreement No 636307. This paper was supported by the János Bolyai Research Scholarship of the Hungarian Academy of Sciences. The research reported in this paper was supported by the Higher Education Excellence Program of the Ministry of Human Capacities in the frame of Artificial Intelligence research area of Budapest University of Technology and Economics (BME FIKPMI/FM).

ORCID

Tamás Baár  <http://orcid.org/0000-0003-0036-4114>

Tamás Luspay  <http://orcid.org/0000-0002-3845-576X>

References

- Apkarian, P., Dao, M. N., & Noll, D. (2015). Parametric robust structured control design. *IEEE Transactions on Automatic Control*, 60(7), 1857–1869. <https://doi.org/10.1109/TAC.2015.2396644>
- Baár, T., & Luspay, T. (2019). An H_2/H_∞ blending for mode decoupling. American control conference (ACC), Philadelphia, PA (pp. 175–180).
- Bakule, L. (2008). Decentralized control: An overview. *Annual Reviews in Control*, 32(1), 87–98. <https://doi.org/10.1016/j.arcontrol.2008.03.004>
- Danowsky, B. P., Thompson, P., Lee, D. C., & Brenner, M. J. (2013). Modal isolation and damping for adaptive aeroservoelastic suppression. AIAA atmospheric flight mechanics (AFM) conference, Boston, MA.
- FLEXOP project (2015). Flutter Free FLight Envelope eXpansion for economical Performance improvement. Retrieved July 23, 2019, from <https://flexop.eu>
- Glover, K., & Varga, A. (2011). On solving non-standard H_2/H_∞ fault detection problems. 2011 50th IEEE conference on decision and control and European control conference, Orlando, FL (pp. 891–896).
- Grigoriadis, K. M., & Beran, E. B. (2000). Alternating projection algorithms for linear matrix inequalities problems with rank constraints. In Laurent El Ghaoui & Silviu-lulian Niculescu (Eds.), *Advances in linear matrix inequality methods in control* (pp. 251–267). SIAM.
- Hamdan, A., & Nayfeh, A. (1989). Measures of modal controllability and observability for first-and second-order linear systems. *Journal of Guidance, Control, and Dynamics*, 12(3), 421–428. <https://doi.org/10.2514/3.20424>
- Iwasaki, T., Meinsma, G., & Fu, M. (2000). Generalized S-procedure and finite frequency KYP lemma. *Mathematical Problems in Engineering*, 6(2–3), 305–320. <https://doi.org/10.1155/S1024123X00001368>
- Kailath, T. (1980). *Linear systems* (Vol. 156). Prentice-Hall.
- Kwakernaak, H., & Sivan, R. (1972). *Linear optimal control systems* (Vol. 1). Wiley-Interscience.
- Li, X., & Liu, H. H. (2010). A necessary and sufficient condition for H_2 index of linear time-varying systems. *49th IEEE conference on decision and control (CDC)*, Atlanta, GA (pp. 4393–4398).
- Lin, C. A., & Wu, C. M. (2001). Decoupling precompensation and optimal decoupling. *Journal of the Chinese Institute of Engineers*, 24(1), 19–28. <https://doi.org/10.1080/02533839.2001.9670602>
- Liu, J., Wang, J. L., & Yang, G. H. (2005). An LMI approach to minimum sensitivity analysis with application to fault detection. *Automatica*, 41(11), 1995–2004. <https://doi.org/10.1016/j.automatica.2005.06.005>
- Löfberg, J. (2004). YALMIP: A toolbox for modeling and optimization in MATLAB. *Proceedings of the CACSD conference*, New Orleans, LA (Vol. 3).
- Luenberger, D. G. (1997). *Optimization by vector space methods*. Wiley.
- Luspay, T., Péni, T., Gözse, I., Szabó, Z., & Vanek, B. (2018). Model reduction for LPV systems based on approximate modal decomposition. *International Journal for Numerical Methods in Engineering*, 113(6), 891–909. <https://doi.org/10.1002/nme.v113.6>
- Luspay, T., Péni, T., & Vanek, B. (2018). Control oriented reduced order modeling of a flexible winged aircraft. *2018 IEEE aerospace conference*, Big Sky, MT (pp. 1–9).
- Marinescu, B. (2009). Model-matching and decoupling for continuous- and discrete-time linear time-varying systems. *International Journal of Control*, 82(6), 1018–1028. <https://doi.org/10.1080/00207170802400962>
- Mohammadpour, J., Grigoriadis, K., Franchek, M., Wang, Y. Y., & Haskara, I. (2011). LPV decoupling for control of multivariable systems. *International Journal of Control*, 84(8), 1350–1361. <https://doi.org/10.1080/00207179.2011.596573>
- Pusch, M. (2018). Aeroelastic mode control using H_2 -optimal blends for inputs and outputs. *2018 AIAA guidance, navigation, and control conference*, Kissimmee, FL (pp. 618–630).
- Pusch, M., & Ossmann, D. (2019). H_2 -optimal blending of inputs and outputs for modal control. *IEEE Transactions on Control Systems Technology*, 1–8. <https://doi.org/10.1109/TCST.87>
- Pusch, M., Ossmann, D., Dillinger, J., Kier, T. M., Tang, M., & Lübker, J. (2019). Aeroelastic modeling and control of an experimental flexible wing. *AIAA scitech 2019 forum*, San Diego, CA (pp. 131–146).
- Pusch, M., Ossmann, D., & Luspay, T. (2019). Structured control design for a highly flexible flutter demonstrator. *Aerospace*, 6(3), 27–47. <https://doi.org/10.3390/aerospace6030027>
- Scherer, C., & Weiland, S. (2000). *Lecture notes: Linear matrix inequalities in control*. Dutch Institute for Systems and Control.
- Skogestad, S., & Postlethwaite, I. (2007). *Multivariable feedback control: analysis and design* (Vol. 2). Wiley.
- Stoyle, P., & Vardulakis, A. (1979). The mechanism of decoupling. *International Journal of Control*, 29(4), 589–605. <https://doi.org/10.1080/0020717908922722>
- Sturm, J. F. (1999). Using SeDuMi 1.02, a MATLAB toolbox for optimization over symmetric cones. *Optimization Methods and Software*, 11(1–4), 625–653. <https://doi.org/10.1080/10556789908805766>
- Wang, Q. G. (2002). *Decoupling control* (Vol. 285). Springer Science & Business Media.
- Wang, H., & Yang, G. H. (2008). A finite frequency domain approach to fault detection observer design for linear continuous-time systems. *Asian Journal of Control*, 10(5), 559–568. <https://doi.org/10.1002/asjc.v10i5>
- Wang, J. L., Yang, G. H., & Liu, J. (2007). An LMI approach to H_2 index and mixed H_2/H_∞ fault detection observer design. *Automatica*, 43(9), 1656–1665. <https://doi.org/10.1016/j.automatica.2007.02.019>
- Zhou, K., & Doyle, J. C. (1998). *Essentials of robust control* (Vol. 104). Prentice Hall.

Appendix 1. Proof of Lemma 2.3

First we consider the case of (7) where the proof is relatively easy. If a symmetric matrix is positive definite, then all the block diagonal terms are positive definite. This immediately results in the inequality of $D^T D > \beta^2 I$ corresponding to the lower right diagonal block of (7). This can only be satisfied if $D^T D$ has full rank, i.e. D has full column rank, and $n_y \geq n_u$. Consequently, if $n_u > n_y$ then the dual representation has to be used for computing the \mathcal{H}_2 index of the system.

Next we investigate the case of (8). The application of Lemma 2.2 resolves necessity of the direct feedthrough, and the \mathcal{H}_2 index can be calculated over a finite frequency range when $D = 0$. However the constraint to the relation of $n_y \geq n_u$ still holds. This can be proven as follows.

The matrix multiplications in (8) can be expanded as

$$M = \begin{bmatrix} M_{11} & M_{12} \\ M_{12}^T & M_{22} \end{bmatrix} < 0, \text{ with}$$

$$M_{11} = -A_c^T Q_c A_c + A_c^T P_c + j A_c^T \tilde{\omega} Q_c + P_c A_c \\ - j \tilde{\omega} Q_c A_c - \underline{\omega} \tilde{\omega} Q_c - C_c^T C_c,$$

$$\begin{aligned} M_{12} &= -A_c^T Q_c B_c + P_c B_c - j \frac{\tilde{\omega}}{2} Q_c B_c - C^T D, \\ M_{22} &= -B_c^T Q_c B_c - D^T D + \beta^2 I, \end{aligned} \quad (A1)$$

where $M \in \mathbb{C}^{(n_x+n_u) \times (n_x+n_u)}$ and M is partitioned as $\begin{bmatrix} n_x \times n_x & n_x \times n_u \\ n_u \times n_x & n_u \times n_u \end{bmatrix}$. Also carry out the multiplications in (8) for the dual representation of the system given by (5) to obtain

$$\begin{aligned} \tilde{M} &= \begin{bmatrix} \tilde{M}_{11} & \tilde{M}_{12} \\ \tilde{M}_{12}^T & \tilde{M}_{22} \end{bmatrix} < 0, \text{ with} \\ \tilde{M}_{11} &= -A_c Q_c A_c^T + A_c P_c + j A_c \frac{\tilde{\omega}}{2} Q_c + P_c A_c^T \\ &\quad - j \frac{\tilde{\omega}}{2} Q_c A_c^T - \underline{\omega} \tilde{\omega} Q_c - B_c B_c^T, \\ \tilde{M}_{12} &= -A_c Q_c C_c^T + P_c C_c^T - j \frac{\tilde{\omega}}{2} Q_c C_c^T - B D^T, \\ \tilde{M}_{22} &= -C_c Q_c C_c^T - D D^T + \beta^2 I, \end{aligned} \quad (A2)$$

where $\tilde{M} \in \mathbb{C}^{(n_x+n_y) \times (n_x+n_y)}$, and \tilde{M} is partitioned as $\begin{bmatrix} n_x \times n_x & n_x \times n_y \\ n_y \times n_x & n_y \times n_y \end{bmatrix}$.

Take the case when $D = 0$. Note again the fact that if a symmetric matrix is positive definite, than its diagonal terms are also positive definite. From (A1) and (A2), we have $M_{22} = -B_c^T Q_c B_c + \beta^2 I < 0$ and $\tilde{M}_{22} = -C_c Q_c C_c^T + \beta^2 I < 0$. Since $Q_c \in \mathbb{C}^{(n_x) \times (n_x)}$, these inequalities can only be satisfied if $n_u \leq n_x$ and $n_y \leq n_x$, respectively.

Next we continue with the more general case, when $D \neq 0$. Suppose that $n_y > n_u$. The proof is based on the following two rank identities

$$\text{rank}(X + Y) \leq \text{rank}(X) + \text{rank}(Y), \quad (A3)$$

$$\text{rank}(XY) \leq \min(\text{rank}(X), \text{rank}(Y)). \quad (A4)$$

The input–output norm equality implies that the term β^2 is the same for both (A1) and (A2), i.e. M_{22} and \tilde{M}_{22} have to satisfy

$$\beta^2 I < B_c^T Q_c B_c + D^T D, \quad (A5)$$

$$\beta^2 I < C_c Q_c C_c^T + D D^T. \quad (A6)$$

The left hand side of (A5) and (A6) are full rank, with ranks n_u and n_y , respectively. According to (A4) and the fact that $Q_c \in \mathbb{C}^{n_x \times n_x}$:

$$\text{rank}(B_c^T Q_c B_c) \leq n_x, \quad \text{rank}(C_c Q_c C_c^T) \leq n_x. \quad (A7)$$

At the same time, we supposed that $n_y \geq n_u$, which implies:

$$\text{rank}(D^T D) = \text{rank}(D D^T) \leq n_u. \quad (A8)$$

So according to (A3) maximal rank of the right hand sides of (A5) and (A6) is $n_x + n_u$.

We can further conclude that the right hand sides of (A5) and (A6) have to be full rank, in order to satisfy the inequalities. However, since they have the same upper bound, it means only the smaller dimensional can hold and the other one on the right hand side will have zero eigenvalues. If $n_y \geq n_u$ than the n_u dimensional equation (A5) is solvable, and so LMI (A1) provides the \mathcal{H}_- index.

It can be easily seen that if $n_y < n_u$ then based on the same reasoning (A6) becomes solvable, and the LMI (A2) corresponding to the dual representation becomes solvable, which is tall. If $n_y = n_u$ than (A1) and (A2) yields the same \mathcal{H}_- index. Therefore, we concluded that the \mathcal{H}_- index can only be calculated for tall or square systems.

Appendix 2. The input blend algorithm

Algorithm 1 Input blend calculation with alternating projection

- 1: **Given:** The subsystems \mathcal{G}_c and \mathcal{G}_d are given in a form as shown in Figure 2.
- 2: **Initialisation:** Solve the following optimisation problem, for $\beta^2, \gamma^2, P_d, P_c, Q, K_u$:

$$\text{minimise}_{P_d, K_u, P_c, Q, \beta^2, \gamma^2} -\beta^2 + \gamma^2 + \text{trace}(K_u)$$

$$\text{s.t.}: \begin{bmatrix} P_d A_d^T + A_d P_d + B_d K_u B_d^T \\ C_d P_d + D K_u B_d^T \end{bmatrix}$$

$$\begin{bmatrix} P_d C_d^T + B_d K_u D^T \\ D K_u D^T - \gamma^2 I \end{bmatrix} \leq 0,$$

$$\begin{bmatrix} A_c^T & C_c^T \\ I & 0 \end{bmatrix}^T \Xi \begin{bmatrix} A_c^T & C_c^T \\ I & 0 \end{bmatrix}$$

$$+ \begin{bmatrix} B_c^T & D^T \\ 0 & I \end{bmatrix}^T \Pi \begin{bmatrix} B_c^T & D^T \\ 0 & I \end{bmatrix} < 0,$$

$$0 \leq K_u \leq I, \quad Q \geq 0.$$

- 3: **for** $k = 1$ to $n_u - 1$ **do**

- 4: $j = 0$

- 5: $K_u^* = \mathcal{P}_{\Gamma_{\text{rank}}^{n-k}} K_u$

- 6: **while** $\frac{|K_{u_{j+1}}^* - K_{u_j}^*|}{|K_{u_j}^*|} > \text{threshold}$ **do**

- 7: Solve the following optimisation problem, for P_c, Q, P_d, S, K_u :

$$\text{minimise}_{P_d, K_u, P_c, Q, S} \text{trace}(S)$$

$$\text{s.t.}: \begin{bmatrix} P_d A_d^T + A_d P_d + B_d K_u B_d^T \\ C_d P_d + D K_u B_d^T \end{bmatrix}$$

$$\begin{bmatrix} P_d C_d^T + B_d K_u D^T \\ D K_u D^T - \gamma^2 I \end{bmatrix} \leq 0,$$

$$\begin{bmatrix} A_c^T & C_c^T \\ I & 0 \end{bmatrix}^T \Xi \begin{bmatrix} A_c^T & C_c^T \\ I & 0 \end{bmatrix}$$

$$+ \begin{bmatrix} B_c^T & D^T \\ 0 & I \end{bmatrix}^T \Pi \begin{bmatrix} B_c^T & D^T \\ 0 & I \end{bmatrix} < 0,$$

$$0 \leq K_u \leq I, \quad Q \geq 0,$$

$$\begin{bmatrix} S & K_u - K_u^* \\ K_u - K_u^* & I \end{bmatrix} \geq 0.$$

- 8: $K_{u_{j+1}}^* = \mathcal{P}_{\Gamma_{\text{rank}}^{n-k}} K_{u_j}^*$

- 9: $j = j + 1$

- 10: **end while**

- 11: **end for**

- 12: Find k_u as the left singular vector corresponding to the largest singular value, from the singular value decomposition $K_u^* = U S V^T$.

Appendix 3. The output blend algorithm

Algorithm 2 Output blend calculation with alternating projection

- 1: **Given:** The subsystems \mathcal{G}_c and \mathcal{G}_d are given in the form of (18), and remove the direct feedthrough.
- 2: **Initialisation:** Solve the following optimisation problem, for $\beta^2, \gamma^2, P_d, P_c, Q, K_y$:

$$\begin{aligned}
 & \text{minimise}_{P_d, K_y, P_c, Q, \beta^2, \gamma^2} -\beta^2 + \gamma^2 + \text{trace}(K_y) \\
 & \text{s.t.} \begin{bmatrix} \bar{A}_d^T P_d + P_d \bar{A}_d + \bar{C}_d^T K_y \bar{C}_d \\ \bar{B}_d^T P_d + \bar{D}_d^T K_y \bar{C}_d \\ P_d \bar{B}_d + \bar{C}_d^T K_y \bar{D}_d \\ \bar{D}_d^T K_y \bar{D}_d - \gamma^2 I \end{bmatrix} \preceq 0 \\
 & \begin{bmatrix} \bar{A}_c & \bar{B}_c \\ I & 0 \end{bmatrix}^T \Xi \begin{bmatrix} \bar{A}_c & \bar{B}_c \\ I & 0 \end{bmatrix} \\
 & + \begin{bmatrix} \bar{C}_c & \bar{D}_c \\ 0 & I \end{bmatrix}^T \Pi \begin{bmatrix} \bar{C}_c & \bar{D}_c \\ 0 & I \end{bmatrix} \prec 0, \\
 & 0 \leq K_y \leq I, Q \geq 0.
 \end{aligned}$$

- 3: **for** $k = 1$ to $n_y - 1$ **do**
- 4: $j = 0$
- 5: $K_y^* = \mathcal{P}_{\Gamma_{\text{rank}}^{n-k}} K_y$
- 6: **while** $\frac{|K_{j+1}^* - K_j^*|}{|K_j^*|}$ **do**
- 7: Solve the following optimisation problem, for P_d, P_c, Q, S, K_y :

$$\begin{aligned}
 & \text{minimise}_{P_d, K_y, P_c, Q, S} \text{trace}(S) \\
 & \text{s.t.} \begin{bmatrix} \bar{A}_d^T P_d + P_d \bar{A}_d + \bar{C}_d^T K_y \bar{C}_d \\ \bar{B}_d^T P_d + \bar{D}_d^T K_y \bar{C}_d \\ P_d \bar{B}_d + \bar{C}_d^T K_y \bar{D}_d \\ \bar{D}_d^T K_y \bar{D}_d - \gamma^2 I \end{bmatrix} \preceq 0 \\
 & \begin{bmatrix} \bar{A}_c & \bar{B}_c \\ I & 0 \end{bmatrix}^T \Xi \begin{bmatrix} \bar{A}_c & \bar{B}_c \\ I & 0 \end{bmatrix} \\
 & + \begin{bmatrix} \bar{C}_c & \bar{D}_c \\ 0 & I \end{bmatrix}^T \Pi \begin{bmatrix} \bar{C}_c & \bar{D}_c \\ 0 & I \end{bmatrix} \prec 0, \\
 & 0 \leq K_y \leq I, Q \geq 0, \\
 & \begin{bmatrix} S & K_y - K_y^* \\ K_y - K_y^* & I \end{bmatrix} \succeq 0.
 \end{aligned}$$

- 8: $K_{j+1}^* = \mathcal{P}_{\Gamma_{\text{rank}}^{n-k}} K_j^*$
- 9: $j = j + 1$
- 10: **end while**
- 11: **end for**
- 12: Find k_y as the left singular vector corresponding to the largest singular value, from the singular value decomposition $K_y^* = USV^T$.